Vector- and tensor-meson production and the Pomeron-f identity hypothesis

S. T. Jones
Department of Physics and Astronomy, The University of Alabama, Tuscaloosa, Alabama 35487
(Received 24 November 1987; revised manuscript received 11 April 1988)

Within the context of a model introduced some time ago, the differential and total production cross sections for vector and tensor mesons are shown to be compatible with the hypothesis that the Pomeron and f are a single Regge trajectory. The model incorporates both cylinder and flavoring renormalizations of the Pomeron-f trajectory. The processes $K^{\pm}p \to K^*(892)^{\pm}p$, $K^{\pm}p \to K_2^*(1430)^{\pm}p$, and $\pi^{\pm}p \to A_2(1320)^{\pm}p$ are analyzed in some detail.

About ten years ago,[1] it was proposed that the Pomeron Regge trajectory was identical to the f trajectory, and that quark diagrams with the topology of the cylinder were responsible for breaking the degeneracy between the f and ρ, A_2, and ω trajectories which exists at the planar level. It was soon pointed out[2] that, because of the breaking of SU(3) symmetry which is demonstrated by total-cross-section data, such a Pomeron would have to couple to processes such as $Kp \to K^*(892)p$. Analysis of these processes in traditional Regge formulations showed the data to be incompatible with a Regge trajectory of intercept 1. The experimental cross sections were too small and fell too rapidly for such a model.

In response to this, the author proposed[3] that the cylinder renormalization of the Pomeron be tied to another effect, called flavoring, which has been studied in some detail.[4] Flavoring is a threshold effect, incorporating through unitarity the effects of $K\bar{K}$ production, $N\bar{N}$ production, etc. Although the flavoring model does *not* contain s-dependent Regge poles, it *can* be characterized in terms of *effective* poles. As a new threshold is crossed ($K\bar{K}$ or $N\bar{N}$, for instance), the intercept of the *effective* pole increases. The flavoring model explains in this way the transition from decreasing total cross sections [$\alpha_{\text{eff}}(0) \sim 0.85$] for $s \leq 200$ GeV^2, to roughly constant total cross sections [$\alpha_{\text{eff}}(0) \sim 1.0$] for $200 \leq s \leq 1000$ GeV^2, and finally to increasing cross sections ($\alpha_{\text{eff}} \sim 1.1$) in the CERN ISR-SPS collider energy regime. It is natural to ask whether such an effect could help explain the energy dependence of K^* (892) production.

A coupled-channel model was introduced in Ref. 3 which showed that flavoring should be considered a nonplanar effect. The important ingredient was that the Pomeron-exchange amplitude behaves as if the Pomeron intercept were 0.85, not 1.0, until moderately high energies. This particular realization of the Pomeron-f identity hypothesis was then shown in fact to be compatible with existing data on total cross sections, the process $\pi p \to \rho p$, and the process of interest, $Kp \to K^*(892)p$. It was noted, however, that the agreement was tenuous in the latter case, and that the data did appear to be falling at a more rapid rate than the model. The importance of data at only slightly high energies (40 GeV/c for K^-p was the highest momentum studied in Ref. 3) was stressed.

It has recently come to the author's attention that data on $K^*(892)$ production are now available at laboratory momenta up to 175 GeV/c (for K^-p). Furthermore, the data now exhibit clear evidence of a diffractive component. For instance, in Ref. 5 the data are compared to the f-dominated Pomeron model,[6] and found to be in good agreement. This model[6] incorporates both an f [$\alpha_f(0) \approx 0.5$] and a Pomeron [$\alpha_p(0) \approx 1.0$] trajectory, but relates the Pomeron coupling explicitly to the SU(3)-flavor-symmetry breaking: that is, to the difference between α_f and $\alpha_{f'}$. It is of interest to investigate whether these new data are also compatible with a model containing only a single vacuum trajectory, that is, where the Pomeron is the f trajectory. The purpose of this paper is to show that not only the $K^*(892)$ data, but also related data on tensor-meson production, are indeed compatible with the Pomeron-f identity hypothesis, as incorporated in the flavoring model of Ref. 3.

We briefly review the model of Ref. 3. The absorptive part of the forward amplitude for elastic scattering is assumed to be given by

$$A(s) = \int \frac{dJ}{2\pi i} s^J A(J) , \tag{1}$$

with the J-plane amplitude determined by unitarity. With a kernel $K(J)$ and propagator $P(J)$, the J-plane amplitude is given by

$$A(J) = \sum_{n=0}^{\infty} \bar{V} P (KP)^n V \tag{2}$$

$$= \bar{V} P (1 - KP)^{-1} V . \tag{3}$$

In the simplest one-channel flavoring model, the propagator P is just $(J - \hat{\alpha})^{-1}$, where $\hat{\alpha}$ is the unflavored Pomeron with $\hat{\alpha}(0) \sim 0.85$. The vertex factors V may be taken to be constants, and K is given by

$$K_1(J) = g e^{-bJ} . \tag{4}$$

The integral in Eq. (1) can be evaluated with this amplitude $A(J)$ in two ways. The first is to sum the contributions from the poles in $(1 - KP)^{-1}$; there is a leading real pole α_P (the flavored Pomeron) and an infinite sequence of complex poles. Asymptotically α_P dominates the amplitude, but at intermediate energies the complex

poles are important.

Equivalently, the amplitude $A(J)$ can be expanded in an infinite sum, Eq. (2), the nth term of which contains an nth-order pole:

$$A_n(J)\sim\frac{g^n e^{-nbJ}}{(J-\hat{\alpha})^n} . \tag{5}$$

Letting $y=\ln(s/s_0)$, Eq. (1) gives

$$A_n(s)\sim g^n e^{(y-nb)\hat{\alpha}}\theta(y-nb) . \tag{6}$$

The θ function arises from the need to close the contour to the right if $y<nb$. The contour c is specified to be to the *right* of the singularities in $A(J)$. Expression (6) clearly exhibits the threshold at $\ln(s/s_0)=nb$ for producing n pairs of heavy particles.

In this paper we consider a two-channel model, the two channels corresponding to the ideally mixed $I=0$ combinations $(u\bar{u}+d\bar{d})/\sqrt{2}$ and $s\bar{s}$, respectively. $V(J)$ then becomes a two-component vector, with a J dependence because we expect different energy thresholds for light and heavy external particles. The propagator $P(J)$ is now a matrix of unflavored trajectories: namely,

$$P(J)=\begin{bmatrix}(J-\alpha_0)^{-1} & 0\\ 0 & (J-\alpha_3)^{-1}\end{bmatrix} . \tag{7}$$

We wish to use the model of Ref. 3 which assumed α_0 and α_3 already contain *all* planar contributions, whether from light or heavy quarks. The cylinder diagrams will break the degeneracy between $I=0$ and $I=1$ trajectories as well as to mix α_0 with α_3. Only cylinder $K\bar{K}$ production will have a threshold factor such as Eq. (4). With these assumptions, the kernel K is also a two-by-two matrix: namely,

$$K^C(J)=C\begin{bmatrix}2k & (2Kk)^{1/2}e^{-bJ}\\ (2Kk)^{1/2}e^{-bJ} & Ke^{-2bJ}\end{bmatrix} . \tag{8}$$

Here $C=\pm1$ is the C parity of the exchanged trajectories, $\sqrt{2k}$ and $\sqrt{K}$ are the cylinder couplings to intermediate mesons of $I=0$ Reggeons with non-strange- and strange-quark contents, respectively, and we have assumed a threshold factor of e^{-bJ} for each strange-quark pair produced in the intermediate state.

The expansion of Eq. (3) takes the following form:

$$A(J)=\bar{V}MV ,$$

where

$$M=P+PKP+PKPKP+\cdots . \tag{9}$$

These first three terms are shown diagrammatically in Fig. 1. The upper and lower diagonal elements give the exchanges which can attach to nonstrange and strange external quarks, at each end, respectively. The off-diagonal elements are appropriate for light quarks scattering off strange quarks. Figure 1 shows how the cylinder diagrams mix the $s\bar{s}$ vacuum trajectory (α_3) and the light-quark vacuum trajectory (α_0) to produce the physical trajectories $\alpha_{f'}$ and α_f. The figure also demonstrates why we expect $s\bar{s}$ production to have a significant threshold energy. In the cylinder diagrams, it is necessary to produce an intervening meson (or equivalently, an $s\bar{s}$ Reggeon, as in the third-order term in Fig. 1) between the s and $\bar{s}$ quarks. As each additional produced particle in a multiperipheral chain requires an average rapidity interval Δy, we see that *two* such intervals are required for $s\bar{s}$ production. The higher mass of the strange mesons is thus not the only reason for a high threshold energy.

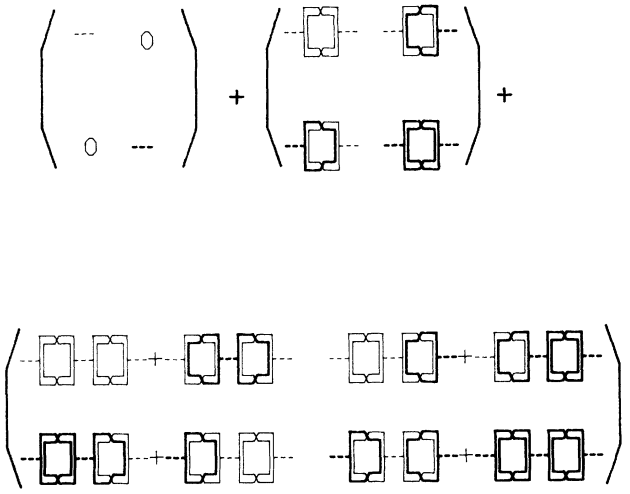

FIG. 1. Diagrammatical representation of the expansion of the forward elastic amplitude. The first three iterations of the expansion are shown. Heavy lines indicate strange quarks, light lines represent light quarks. The rows and columns of the matrix are labeled by $(u\bar{u}+d\bar{d})/\sqrt{2}$ and $s\bar{s}$, respectively.

In the Pomeron-f identity model, the nonstrange component of the cylinder (the upper-left term in K^C) is assumed to break the degeneracy of the f and f', boosting the f up to $\hat{\alpha}_f$, with an intercept of about 0.85. We divide $K^{\pm}(J)$ into light- and heavy-quark contributions: namely,

$$K^{\pm}(J)=K_0^{\pm}(J)+K_3^{\pm}(J) , \tag{10}$$

where

$$K_0^{\pm}(J)=\pm\begin{bmatrix}2k & 0\\ 0 & 0\end{bmatrix} . \tag{11}$$

We can now sum the light-quark contributions to get

$$A(J)=\bar{V}\hat{P}(1-K_3\hat{P})^{-1}V , \tag{12}$$

where

$$\hat{P}=\begin{bmatrix}(J-\hat{\alpha}_f)^{-1} & 0\\ 0 & (J-\hat{\alpha}_3)^{-1}\end{bmatrix} . \tag{13}$$

The exchanged trajectories are given by the poles of $A(J)$. Because of the threshold factors e^{-bJ}, we find both real poles (the Pomeron, $f',\omega,\phi,\ldots$) and complex poles. At very high energies, the real poles dominate the amplitude; at lower energies, the complex pole contributions describe the threshold effects.

The amplitude for vector- and tensor-meson production is now obtained by giving K and k a linear t dependence (see Table I), and by inserting appropriate vertex factors. We use

TABLE I. (a) Parameters determined by total-cross-section and vector-meson fits (Ref. 3). (b) Parameters determined by fits to tensor-meson data (this paper).

(a)		
$\beta^+=11.2$ GeV$^{1/2}$	$K(t)=2.44-1.5t$	$B=0.22$
$\beta^-=10.85$ GeV$^{1/2}$	$k(t)=0.125-0.2t$	$b=0.98$
$\hat{\alpha}_f(t)=0.85+0.6t$		$\gamma^+=1.05$ GeV^{-2}
$\hat{\alpha}_\omega(t)=0.35+1.4t$		$\gamma^-=3.0$ GeV^{-2}
$\alpha_3(t)=0.2+t$		$\bar{g}=0.89$ GeV$^{1/2}$
(b)		
$\bar{g}=0.206$ GeV$^{1/2}$	$\beta_\rho=0.21$ GeV	$\beta_\pi=67.8$ GeV^{-1}
$\gamma^+=1.60$ GeV^{-2}	$\gamma_\rho=4.51$ GeV^{-2}	$\gamma_\pi=3.43$ GeV^{-2}
$\gamma^-=6.41$ GeV^{-2}		

$$V_{\pi\pi^*}=\bar{g}\begin{bmatrix}1\\0\end{bmatrix}, \tag{14a}$$

$$V^C_{NN}=\beta^C e^{-BJ}\begin{bmatrix}1\\0\end{bmatrix}, \tag{14b}$$

$$V_{KK^*}=\bar{g}\begin{bmatrix}\frac{1}{2}\\ \pm 1/\sqrt{2}\end{bmatrix}. \tag{14c}$$

Here π^* represents $(\pi, A_2, \ldots)$ while K^* represents $(K, K^*(892), K_2^*(1430), \ldots)$. The sign of the lower term in V_{KK^*} matches the C parity of the multiplet to which the strange meson belongs. The final detail is to give t dependence to the vertices and to determine the phase of the amplitudes by inserting the appropriate signature factor. The detailed amplitudes are given in the Appendix. It should be noted that in this model the $I=1$ trajectories are unaffected by the cylinder and therefore do not undergo flavoring. They are then represented by conventional Regge-exchange formulas. The parameters b and B, which govern the threshold energy, and k and K, which determine the strength of the $K\bar{K}$ kernel, are determined by fits to total-cross-section data, as are the nucleon couplings $\beta^\pm$. As a result, the only free parameters in the $I_t=0$ amplitudes are the overall coupling $(\bar{g}\beta)$ and the exponential slopes in the t dependence of the couplings for $C=\pm(\beta^C\rightarrow\beta^C e^{-\gamma_c t})$. The amplitude is represented as a sum of the contributions from the poles in A. The leading real poles are the Pomeron, the f' (which is dominantly $s\bar{s}$ in quark content), and the ω. These poles and the complex poles are listed in Table II of Ref. 3. Of particular interest are the Pomeron-f, $\alpha_f(t)=1.02+0.23t$, the f', $\alpha_{f'}(t)=0.49+0.89t$, and the ω, $\alpha_\omega(t)=0.53+0.96t$. The ϕ trajectory is not well treated by the model and is omitted. The $I=1$ trajectories were not needed in Ref. 3; in our analysis of the tensor production processes, we find it advantageous to include these lower-lying trajectories.

Using this model, with the parameters the same as in Ref. 3 [see Table I(a)], we have evaluated the integrated cross sections for $K^\pm p\rightarrow K^*(892)^\pm p$ up to the highest energies for which experimental data is available. The results are shown in Fig. 2, and are clearly in good agreement with the data. We stress that this is a prediction of the model in Ref. 3, using the same parameters determined by the lower-energy fit. This confirms the importance of a Pomeron component, and demonstrates that a model with a single vacuum trajectory (the Pomeron-f identity hypothesis) is compatible with the data.

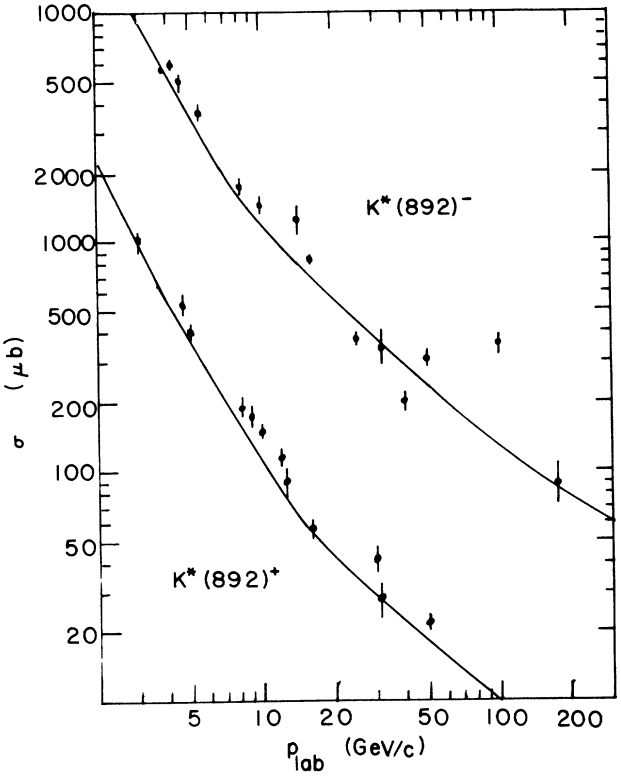

FIG. 2. Integrated cross sections as a function of laboratory momentum for $K^+p\rightarrow K^*(892)^+p$ and $K^-p\rightarrow K^*(892)^-p$. Solid curves are from the model of Ref. 3. The data are from Ref. 6 of this paper and from Ref. 13 of Ref. 3.

For $K^*(1430)$ production, the amplitude is given by the contributions of the Pomeron, ω, f', and π trajectories. We include π exchange in order to fit the rapidly decreasing cross section at lower energies. Omission of the π trajectory leads to a much more nearly constant energy dependence both in this model and in the f-dominated Pomeron model.[6] The Pomeron, f', and ω amplitudes are given by the equations in the Appendix, with the parameters listed in Table I. While one might think that the f', with intercept 0.5, might mock the f contribution in a more conventional model, this is not so. The f' couplings are fixed by the model; the $f'\pi A_2$ and $f'NN$ couplings are small, due to the predominant $s\bar{s}$ content of the f'.

The π amplitude is given by

$$A_\pi(t)=-t\sqrt{-t}\,\beta_\pi e^{\gamma_\pi t}\xi_+(\alpha_\pi(t))(s/s_0)^{\alpha_\pi(t)}, \tag{15}$$

with

$$\xi_\pm(\alpha)=-(e^{-i\pi\alpha}\pm 1)/\sin(\pi\alpha) \tag{16}$$

and

$$\alpha_\pi(t) = -0.02 + t \ . \tag{17}$$

The extra factor of $(-t)$ in (11) is to make the amplitude turn over sufficiently at $t=0$. For the process $\pi p \to A_2(1320)p$, we have contributions from the Pomeron f', and ρ trajectories. The ρ amplitude is given by

$$A_\rho(t) = \sqrt{-t}\,\beta_\rho e^{\gamma_\rho t}\xi_-(\alpha_\rho(t))(s/s_0)^{\alpha_\rho(t)} \ , \tag{18}$$

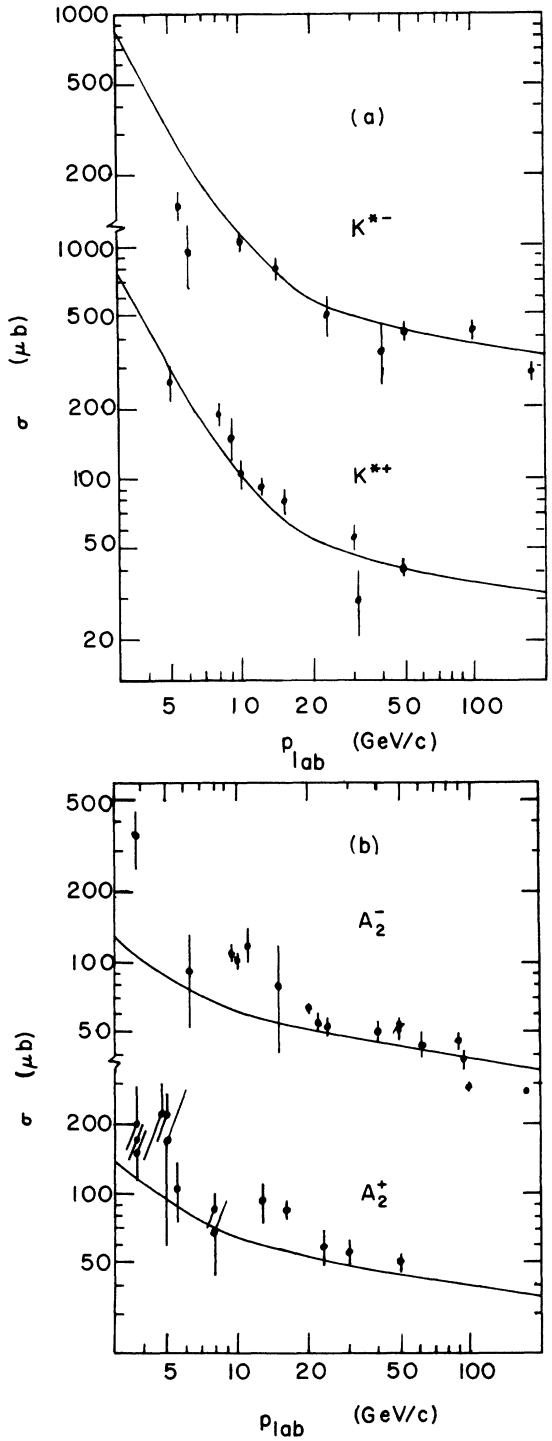

FIG. 3. Integrated cross sections as a function of laboratory momentum for (a) $K^\pm p \to K^*(1430)^\pm p$ and (b) $\pi^\pm p \to A_2(1320)^\pm p$. The solid curves are from the model described in the text. Data are from Refs. 6 and 7.

with

$$\alpha_\rho(t) = 0.6 + t \ . \tag{19}$$

The scale s_0 is 1.0 GeV^2 in these and the other amplitudes.

There are now seven free parameters to be varied in order to fit the $K^*(1430)$ and $A_2(1320)$ data. Although this sounds like a large number of parameters, it is worth noting that (a) the relative couplings of the Pomeron, f', and ω are fixed by the model, and (b) the ρ contribution to $A_2(1320)$ production is very small. There is, then, a strong correlation between the A_2 and K^* amplitudes in this model, especially at higher energies where the π contribution to the K^* amplitude has died out.

The fits achieved with this model are shown in Figs. 3 and 4. The parameters used are listed in Table I. Figure 3 gives the energy dependence of the cross sections, which was the primary concern in determining parameters, while Fig. 4 shows representative differential cross sections. It can be seen that the agreement in the energy dependence (Fig. 3) is rather good, with some exceptions (notably the low-energy A_2^- cross section). A slowly falling Pomeron component is definitely needed. The agreement is not perfect, but is similar to what one achieves with the f-dominated Pomeron model. There is, of course, a fair amount of scatter in the data, due to varying background assumptions, branching ratios assumed, etc.

In Fig. 4 are shown typical differential cross sections. Only limited data on A_2 differential cross sections are available in published form, and we show only the higher-energy cross sections, where the normalization is satisfactory. The shapes of these K^* and A_2 differential cross sections are in satisfactory agreement with the data, although the agreement is better at higher energies.

We summarize by reiterating the main conclusions of this work. We have shown here that a Pomeron component *is* necessary in order to understand vector- and tensor-meson production cross sections. This was first suggested in Ref. 3, and is now corroborated by the higher-energy data. This Pomeron component may be *in addition* to an f component, as in the f-dominated Pomeron model, or it may be the *only* leading vacuum contribution, as in the present model. There is sufficient leeway in each model that neither can be ruled out by the data. The Pomeron-f identity model does have an added consistency check, however, in that it is constrained to fit strange-particle multiplicities in NN scattering. This is the "flavoring" phenomenon. This check is not built into other models. The present work has shown that flavoring, in the context of the dual topological Pomeron, is consistent with vector- and tensor-meson production.

Programming assistance from Don Rockwell is gratefully acknowledged. This work was supported in part by U.S. Department of Energy Grant No. DE-FG05-84014.

APPENDIX

We list here the formulas used in computing the differential tensor-meson cross sections. These are essen-

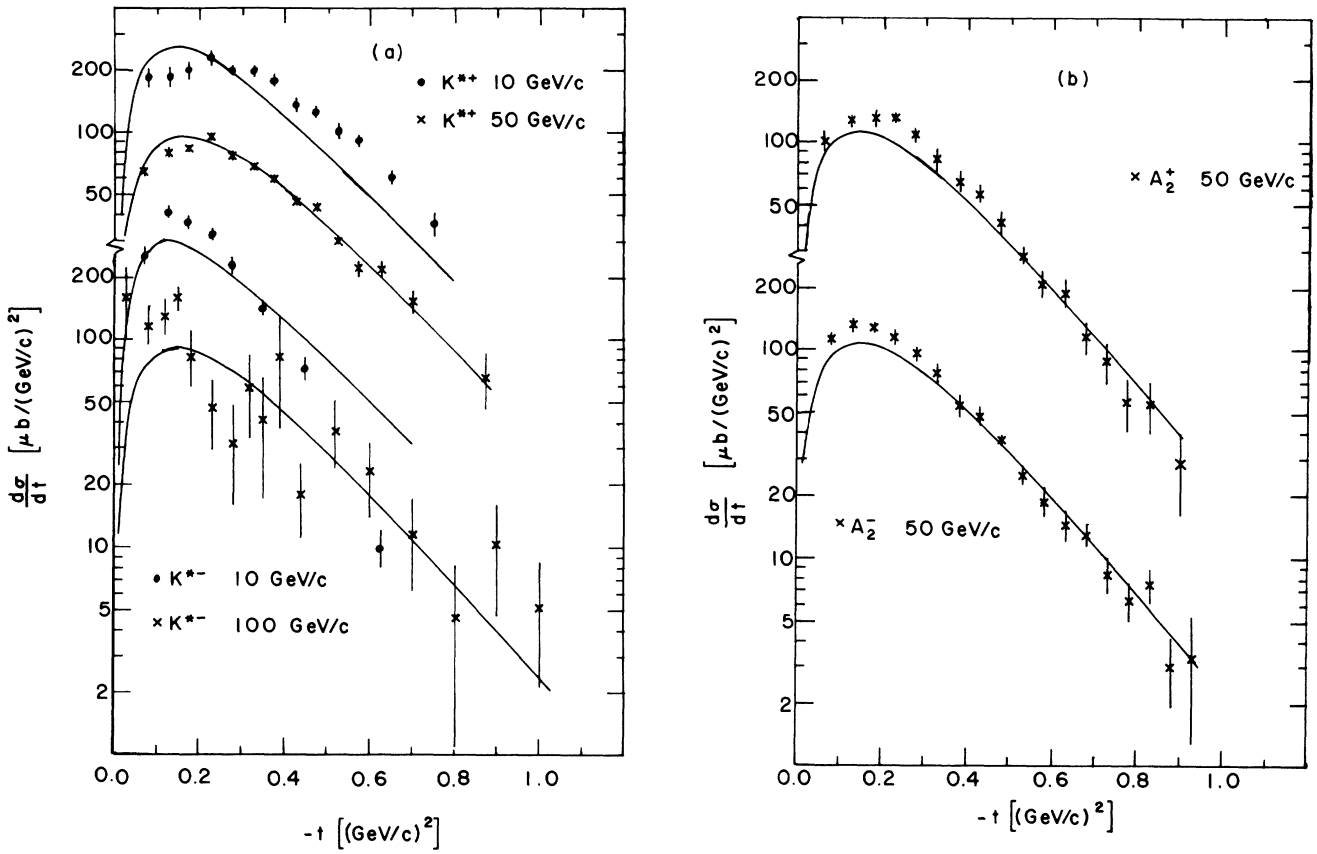

FIG. 4. Representative differential cross sections for (a) $K^{\pm}p \to K^*(1430)^{\pm}p$ and (b) $\pi^{\pm}p \to A_2(1320)^{\pm}p$. The laboratory momenta are indicated. The solid curves are from the model described in the text. Data are from Refs. 6 and 7. In cases where differential-cross-section data were given only for a given channel, the data have been scaled to agree with the cross sections used in Fig. 3.

tially the same as the Appendix to Ref. 3.

The invariant amplitude is given as

$$T(s,t)=\int \frac{dJ}{2\pi i}\xi(J)e^{Jy}A(J,t) \tag{A1}$$

with

$$\xi(J)=-(e^{-i\pi J}\pm 1)/\sin\pi J \ . \tag{A2}$$

K, k, $\hat{\alpha}$, and α_3 are given t dependence as described in the text. Then we write

$$A(J,t)=N(J,t)/D(J,t) \ , \tag{A3}$$

with

$$D(J,t)=(J-\alpha_3)(J-\hat{\alpha})-C(J-\hat{\alpha})Ke^{-2bJ} -2Kke^{-2bJ} \ . \tag{A4}$$

$A(J,t)$ has poles at the zeros of $D(J,t)$. Near a pole at $J=\alpha$, we write

$$D(J,t)\approx(J-\alpha)D'(\alpha) \ , \tag{A5}$$

where

$$D'(\alpha)=\left.\frac{\partial D}{\partial J}\right|_{J=\alpha} \ . \tag{A6}$$

Then

$$T(s,t)=\sum_i \xi(\alpha_i)e^{\alpha_i y}N(\alpha_i)/D'(\alpha_i) \ , \tag{A7}$$

where $y=\ln(s/1\ \mathrm{GeV}^2)$.

The numerator functions for vector- and tensor-meson production are

$$N^{(\alpha)}_{\pi N\to AN}=\bar{g}\beta^C\sqrt{-t}\,e^{-B\alpha}(\alpha-\alpha_3-CKe^{-2b\alpha})e^{\gamma^C t} \tag{A8}$$

and

$$N^{(\alpha)}_{KN\to K^*N}=\bar{g}\beta^C\sqrt{-t}\,e^{-B\alpha} \times[(\alpha-\alpha_3-CKe^{-2b\alpha})/2\pm C\sqrt{kK}\,e^{-b\alpha}]e^{\gamma^C t} \ . \tag{A9}$$

In these formulas, C stands for the C parity of the exchanged pole. The sign of the last term in (A9) matches the C parity of the multiplet to which the K^* belongs [i.e., + for $K, K^*(1430)$, and − for $K^*(892)$]. For the f' amplitude, β is replaced by $\beta\Gamma(\alpha(0))/\Gamma(\alpha(t))$, to cancel the effect of the ghost at $\alpha=0$.

If N^C represents the amplitude due to a pole of C pari-

ty C, then the amplitudes for positively and negatively charged mesons are

$$N_{K^{\pm}}=N^{+}\mp N^{-} \tag{A10}$$

and

$$N_{A^{\pm}}=N^{+}\pm N^{-} \ . \tag{A11}$$

Finally, the differential cross section is given by

$$\frac{d\sigma}{dt}=\frac{0.389}{q^2 s}\,|\,T^2\,|\ . \tag{A12}$$

[1]G. F. Chew and C. Rosenzweig, Phys. Rev. D **12**, 3907 (1975); P. Stevens, G. F. Chew, and C. Rosenzweig, Nucl. Phys. **B110**, 355 (1976).

[2]D. W. Duke, Phys. Lett. **71B**, 347 (1977); C.-I Tan, D. Tow, and J. Tran Thanh Van, *ibid.* **74B**, 115 (1978).

[3]S. T. Jones, Phys. Rev. D **19**, 2792 (1979).

[4]J. Dash, S. T. Jones, and E. Manesis, Phys. Rev. D **18**, 303 (1978).

[5]W. E. Cleland *et al.*, Nucl. Phys. **B208**, 189 (1982); C. Bromberg *et al.*, Phys. Rev. D **29**, 2469 (1984).

[6]R. Carlitz *et al.*, Phys. Rev. D **4**, 3439 (1971).

[7]Data are from Ref. 6 and from A. D. Martin *et al.*, Nucl. Phys. **B134**, 392 (1977); B. Hyams *et al.*, *ibid.* **B146**, 303 (1978); W. E. Cleland *et al.*, *ibid.* **B208**, 228 (1982); and A. D. Martin *et al.*, *ibid.* **B140**, 158 (1978).